

Amphiphilic Copolymers of Acrylic Acid and *n*-Butyl Acrylate with the Predetermined Microstructure: Synthesis and Properties

Yu. V. Levina^a, A. V. Plutalova^b, S. D. Zaitsev^c, R. V. Toms^a, N. S. Serkhacheva^a,
E. A. Lysenko^b, and E. V. Chernikova^{b,*}

^a Lomonosov Institute of Fine Chemical Technologies, Russian Technological University (MIREA), Moscow, 119571 Russia

^b Faculty of Chemistry, Moscow State University, Moscow, 119991 Russia

^c Nizhny Novgorod State Technical University, Nizhny Novgorod, 603950 Russia

*e-mail: chernikova_elena@mail.ru

Received December 18, 2019; revised January 18, 2020; accepted February 3, 2020

Abstract—Features of the synthesis of *n*-butyl acrylate copolymers with acrylic acid in 1,4-dioxane by free radical reversible addition-fragmentation chain transfer (RAFT) polymerization mediated by symmetric trithiocarbonates are considered. It is shown that the living mechanism of polymerization is realized in the studied systems. The chemical nature of the RAFT agent dictates different chain microstructures (random block or random) of the copolymers. The effect of chain microstructure on the properties of the copolymers containing about 90 mol % of acrylic acid units is studied by differential scanning calorimetry, contact angle measurements, turbidimetry, potentiometric titration, and dynamic light scattering. It is demonstrated that all the copolymers in the solid phase have similar properties: a single glass transition temperature close to the glass transition temperature of polyacid and a good water wettability. In dilute aqueous solutions, the properties of the copolymers are different: at the inherent pH, random copolymer macromolecules form large associates, while random block copolymers are dispersed into individual coils or micelles. All the copolymers are weaker polyacids compared with PAA; the random block copolymers are characterized by the compaction of macromolecules at small degrees of ionization. Our studies provide evidence that reversible addition-fragmentation chain transfer polymerization is an efficient tool for the targeted insertion of nonpolar units into a polyelectrolyte chain and it can be used for the fine-tuning of its properties.

DOI: 10.1134/S1560090420030100

INTRODUCTION

Polyelectrolytes form a large and important class of functional polymeric materials. Owing to the chain structure and multicharge state, polyelectrolytes show a number of unique properties: water solubility and ability to interact with charged particles and surfaces and to change the activity of biological objects [1, 2]. At present, polyelectrolytes and their complexes have found wide use as dispersing agents, emulsion and foam stabilizers, structuring agents for soils and grounds, and coagulants and flocculants in wastewater treatment [2–4].

The incorporation of nonpolar units into polyelectrolyte macromolecules renders them amphiphilic and makes it possible to impart a complex of new properties to them, for example, surface activity and ability to interact with nonpolar particles and to change the rheological properties of aqueous solutions [5]. The appearance of new properties is largely associated with a change in the conformational and aggregative states of polyelectrolyte chains caused by the hydrophobic association of nonpolar units. The character of association of hydrophobic units is in turn determined by

their total content and chain microstructure, that is, the sequence of alternation of ionic and nonpolar units [6].

In general, the association of nonpolar units of random copolymers is described by the open association model [7]. In dilute solutions, coils maintain individuality and undergo compaction owing to the intra-chain association of nonpolar units, while in semidilute solutions intermacromolecular association and formation of large particles from many macromolecules take place. For ionic amphiphilic block copolymers, the closed association model holds [8]; micelles composed of the hydrophobic core and ionic corona are formed in solutions. The association of hydrophobic units of random block copolymers occurs within the framework of both models simultaneously [9].

Thus, the controlled synthesis of amphiphilic polyelectrolytes with the predetermined composition and microstructure provides a way to substantially modify the properties of common polyelectrolytes; therefore, this is an urgent issue. A promising tool for tackling this issue is the reversible addition-fragmentation chain transfer (RAFT) polymerization. This method is

attractive because of its simplicity, tolerance to the chemical nature of functional groups of comonomers, and the ability to target the microstructure of the growing chain (random, gradient, or block).

Previously, we reported on the synthesis of a number of ionic amphiphilic copolymers of various composition and microstructure from styrene and acrylic acid and 2,2,3,4,4,4-hexafluorobutyl acrylate, 2,2,3,3,4,4,5,5-octafluoropentyl acrylate, and acrylic acid as comonomers with the use of trithiocarbonates as RAFT agents [10–13]. It was shown that the relative reactivity of the comonomers is determined by the polarity of the solvent and the polarity and nature of the RAFT agent. Regardless of the comonomer mixture composition, products of the desired molecular weight and a fairly narrow molecular weight distribution are formed.

This study addresses the possibility of using RAFT polymerization for the synthesis of copolymers of different microstructure (random and random block) on the basis of heteropolar monomers, acrylic acid (AA) and *n*-butyl acrylate (BA). These monomers are chosen because of their accessibility and a wide application of respective homopolymers in practice. In our study, we will limit ourselves to the case of predominance of AA units and will consider various variants of the distribution of BA and AA units along chain. In the course of presentation, we will successively discuss the synthesis of three types of copolymers (random AA/BA, random block PAA-*block*-P(AA/BA)-*block*-PAA, and PBA-*block*-P(AA/BA)-*block*-PBA) of close composition and comparable MW and will compare their properties in the solid phase in the absence of water and in dilute aqueous solutions/dispersions. The goal of this approach is to understand how the conformational and aggregative behavior of a “common” polyelectrolyte and the complex of its properties can be changed with the use of small additives of hydrophobic units by varying the character of their arrangement along the chain.

EXPERIMENTAL

Acrylic acid and DMF (both from Aldrich) and *n*-butyl acrylate and 1,4-dioxane (both from Acros) were distilled before use. AIBN was recrystallized two times from ethanol and dried in vacuum to a constant weight. Dibenzyl trithiocarbonate (BTC) was synthesized according to the known technique and characterized by NMR spectroscopy, as described in [14].

For the synthesis of poly(*n*-butyl acrylate) trithiocarbonate (PBATC), a solution of AIBN (10^{-3} mol/L) and BTC (0.2 mol/L) in the freshly distilled BA was prepared. In a similar manner for the synthesis of poly(acrylic acid) trithiocarbonate (PAATC), the weighed portions of the initiator (10^{-3} mol/L of AIBN) and the RAFT agent (0.1 mol/L of BTC) were dissolved in a mixture of the freshly distilled AA and

1,4-dioxane taken in equal volumes. The reaction mixtures were poured in 5-mL ampoules, and the ampoules were outgassed on a vacuum setup to a residual pressure of 5×10^{-3} mmHg by repeating freeze–thaw–pump cycles and sealed. Polymerization was conducted at 80°C for 24 h. Afterwards, the ampoules were opened and the reaction mixture was diluted with benzene or 1,4-dioxane and lyophilized. The molecular weight characteristics of the synthesized polymeric RAFT agents were determined by GPC: for PBATC, $M_n = 3.2 \times 10^3$ and $D (M_w/M_n) = 1.31$; for PAATC, $M_n = 5.5 \times 10^3$ and $D = 1.15$.

For the synthesis of BA–AA copolymers, reaction mixtures with a molar ratio of the comonomers from 0 to 100% were prepared. The calculated amounts of the initiator (AIBN, 10^{-3} mol/L) and the RAFT agent (BTC, PBATC, or PAATC, 10^{-2} mol/L) were dissolved in the monomer mixture, and, if necessary, a solvent (1,4-dioxane or DMF) was added. The finished mixtures were poured in ampoules, degassed, and polymerized at 80°C for the predetermined time. When determining the reactivity ratios, the time of polymerization was chosen so that the total conversion of the comonomers did not exceed 10%. Once the reaction was completed, the copolymers were lyophilized. The conversion of the monomers was determined gravimetrically. When BTC was used, the conversion was calculated as the ratio between the weight of the polymer and the weight of the comonomers taken for copolymerization. When using polymeric RAFT agents, the conversion was determined from the ratio of the weight of the grown polymer, that is, the weight of the polymer minus the weight of the polymeric RAFT agent, to the weight of the comonomers.

To prepare the aqueous solutions of the copolymers, the weighed portion of the copolymer was dissolved in 1,4-dioxane to obtain a solution with a polymer concentration of 30 g/L. The solution was diluted with distilled water almost threefold by adding water dropwise under continuous stirring, and the resulting mixture was stirred for 20 h. The obtained solutions were placed in dialysis bags and dialyzed against water for 72 h; the water was changed initially every 6 h and then every 12–15 h. After dialysis, the solution was reconcentrated through the partial evaporation of water on a rotor evaporator. To determine the polymer concentration, a small amount of the solution of the desired volume was sampled and weighed and the polymer was lyophilized and weighed.

The molecular weight characteristics of the synthesized copolymers were estimated by GPC using a DMF solution containing 0.1 wt % LiBr. The measurements were conducted at 50°C on a PolymerLabs GPC-120 chromatograph equipped with two PLgel 5 μ m MIXED B ($M = (5 \times 10^2) - (1 \times 10^7)$) columns and a differential refractometer. Narrowly dispersed PMMA standards were used for calibration. The

copolymers containing AA units were preliminarily methylated by trimethylsilyldiazomethane.

The composition of the copolymers was determined by ^1H NMR spectroscopy on a VARIANXR-400 spectrometer at 400 MHz using DMSO-d_6 as an internal standard. The composition of the copolymers was calculated from the integrated intensities of signals due to one proton of the carboxyl group of AA (16.72 ppm) and three protons of the methyl group of BA (3.0 ppm). The weight fraction of AA units in the copolymer was also estimated by conductometric titration with the aid a TV-6L1 high-frequency titrator. The acetone–ethanol (1 : 1, vol/vol) copolymer solutions were titrated with 0.1 M KOH methanol solution at room temperature; the titration jump was estimated from the point of interception of straight lines on the conductivity versus titrant volume plot.

The potentiometric titration of 1% copolymer aqueous solutions was carried out at room temperature using a HANNA Instruments pH meter; the turbidimetric titration was performed using a KFK-3-01-ZOMS photometer at a wavelength of 579.6 nm. A cuvette with distilled water was placed in a reference cell.

Thermograms of the copolymers were measured on a Netzsch DSC 204 differential scanning calorimeter in a dry argon atmosphere at a flow rate of 100 mL/min in the range of -100 to $+150^\circ\text{C}$ at a heating rate of $10^\circ\text{C}/\text{min}$. The measurements were performed using weighed portions of 4–6 mg; the polymer sample was placed in a standard aluminum crucible with a punctured cover. Thermograms were registered in the third heating–cooling–heating cycle.

The experimental data were treated using the Netzsch Proteus program.

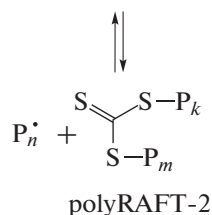
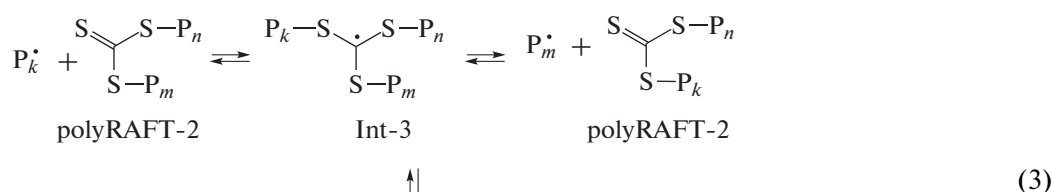
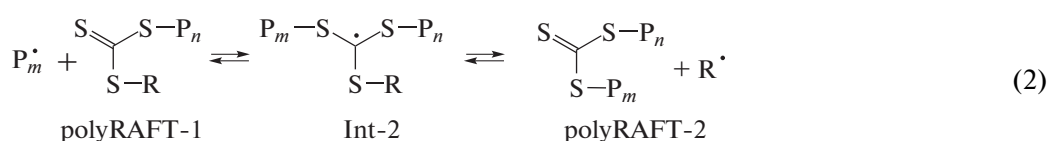
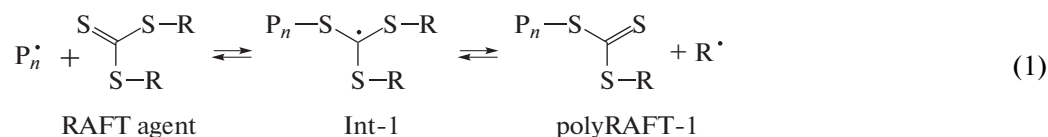
The contact angles were measured by applying the aqueous solutions of the copolymers (1 wt %) as a thin even layer on a fluoroplastic or glass substrate. Substrates with the applied solution were dried in an Axis AGS-200 moisture analyzer to a constant weight and cooled to room temperature. Micrographs were taken with the aid of a video camera coupled with a Dino-Lite AM-411T digital microscope. A water droplet was applied on the substrate with the polymer coating using a syringe with a thin needle. The resulting images were treated with the help of the DinoCapture 2.0 software program.

The average diameter of copolymer particles was measured on a Malvern Zetasizer Nano ZS laser analyzer in the automatic regime at an angle of 90° at a constant temperature of 25°C ; the measurement results were treated using the dedicated software.

RESULTS AND DISCUSSION

*Copolymerization of Acrylic Acid and *n*-Butyl Acrylate Mediated by Dibenzyl Trithiocarbonate*

Previously, RAFT polymerization showed its efficiency in the controlled synthesis of PBA, PAA, and their block copolymers: symmetric trithiocarbonates, for example, BTC, were the most suitable for their synthesis [15–20]. In this case, the RAFT process occurs by the three-stage mechanism (reactions (1)–(3)) and leads to the formation of macromolecules containing trithiocarbonate fragments within chains.



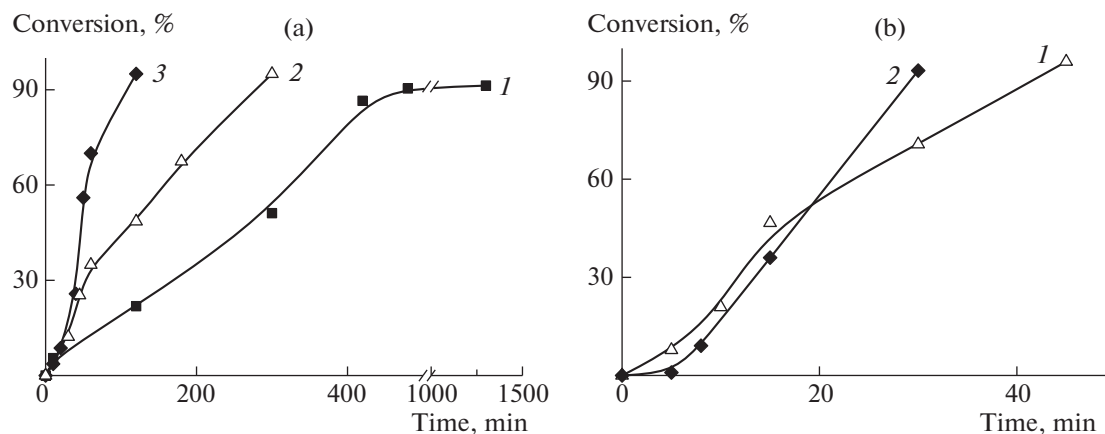


Fig. 1. Time dependences of conversion for the copolymerization AA and BA in various media at $[AIBN] = 10^{-3}$ mol/L and $[BTC] = 10^{-2}$ mol/L; 80°C . (a) Molar ratios of AA : BA = 68 : 32 and AA : solvent = 1 : 1; (1) in bulk, (2) 1,4-dioxane, and (3) DMF; (b) molar ratios of AA : BA = 90 : 10 and AA : solvent = 1.0 : 1.5; (1) 1,4-dioxane and (2) DMF.

It could be expected that BTC would be efficient in the copolymerization of this monomer pair. Figure 1 presents the kinetic curves for the copolymerization of AA and BA in various media at two monomer feed compositions. It is seen that copolymerization in bulk proceeds at a lower rate than that in solution. For solution copolymerization, the reaction kinetics remains unchanged to a monomer conversion of about 30%; afterwards, copolymerization in 1,4-dioxane is retarded compared with the process conducted in DMF. The observed effects may be associated with a change in the relative reactivity of the comonomers in the studied systems (see below), as is typical of heteropolar monomers polymerizing in media with different polarity [21].

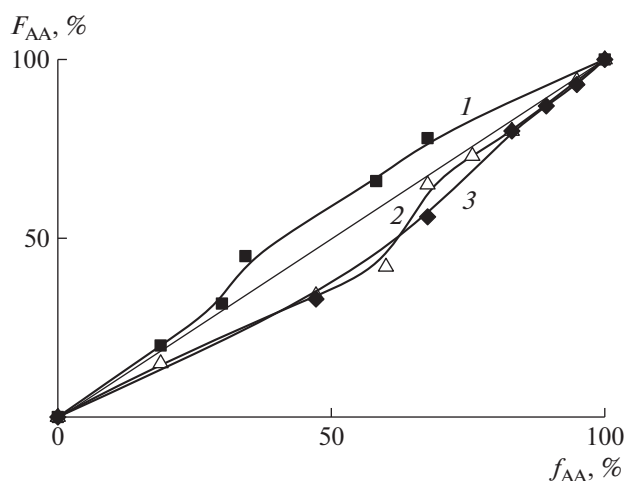


Fig. 2. Phase diagrams of the AA–BA copolymers in (1) bulk, (2) 1,4-dioxane, and (3) DMF. $[AIBN] = [BTC]_0 = 10^{-3}$ mol/L.

The relative reactivities of the comonomers were analyzed by studying the composition of the copolymers formed at initial conversions (below 10%). As is seen from the diagram (Fig. 2), the copolymers produced by bulk copolymerization are enriched in AA units, as opposed to the copolymers synthesized in 1,4-dioxane or DMF, which are enriched in BA units at any monomer feed composition.

The reactivity ratios were calculated by the graphical method (the Fineman–Ross procedure) and the analytical method (linearization by the least squares method, LSM). As follows from Table 1, in bulk copolymerization, AA is more active than BA, while in solution copolymerization the reverse situation is observed. Moreover, the reactivities of the comonomers in 1,4-dioxane and DMF are similar. Hence, it may be anticipated that the compositions of the copolymers synthesized at various conversions in these solvents will be similar.

Thus, difference in the kinetics of copolymerization, as expected, is associated with different reactivities of the comonomers. In bulk copolymerization, AA is a more active monomer, for which the propagation rate constant is an order of magnitude smaller than that for BA [22]. The probability of its occurrence at the end of the growing chain at the chosen feed compositions is higher than that of BA. In solution copolymerization, BA is a more active monomer; as a result, the rate of reaction increases. Once a conversion of 30% is reached, the rate of copolymerization in 1,4-dioxane decreases with that in DMF. The reason for this phenomenon is unclear and calls for further studies.

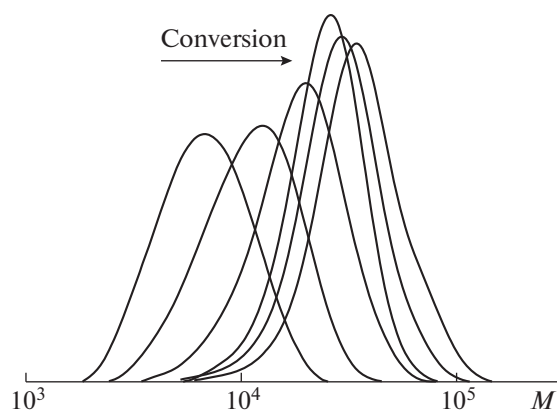
An analysis of the molecular weight characteristics of the copolymers indicates that the nature of the reaction medium has no effect on realization of the RAFT mechanism. As an example, Fig. 3 shows the GPC curves of the copolymers synthesized by copolymer-

Table 1. Relative reactivities of comonomers AA and BA in the BTC-mediated copolymerization in bulk, 1,4-dioxane, and DMF

Medium	LSM	Fineman–Ross method
Bulk	$r_{AA} = 1.91 \pm 0.56$	$r_{AA} = 1.88 \pm 0.63$
	$r_{BA} = 1.06 \pm 0.15$	$r_{BA} = 1.05 \pm 0.23$
1,4-dioxane	$r_{AA} = 0.82 \pm 0.05$	$r_{AA} = 0.69 \pm 0.15$
	$r_{BA} = 1.48 \pm 0.36$	$r_{BA} = 1.31 \pm 0.12$
DMF	$r_{AA} = 0.79 \pm 0.01$	$r_{AA} = 0.86 \pm 0.08$
	$r_{BA} = 2.0 \pm 0.5$	$r_{BA} = 2.30 \pm 0.24$

ization in 1,4-dioxane at a molar content of AA in the monomer feed of 90%. For all the studied systems, the copolymers are characterized by a unimodal MWD, and with an increase in conversion, the curves successively shift to high molecular weights.

Regardless of the monomer feed composition at a constant concentration of the monomers and BTC, all the experimental values of M_n can be described by a single rectilinear dependence (Fig. 4a). The M_n of the copolymers increases in proportion to an increase in the concentration of the monomer. A comparison between the experimental results and the theoretical values is hardly possible, because the values of MW are calculated according to PMMA standards and the values of parameter a in the Kuhn–Mark–Houwink equation for the AA–BA copolymers in DMF solution are unknown. Nevertheless, a linear growth of MM with an increase in conversion is one of the main arguments that polymerization proceeds by the RAFT mechanism.

**Fig. 3.** Unit area normalized GPC curves of the AA–BA copolymers synthesized by copolymerization. $[AIBN] = 10^{-3}$ mol/L and $[BTC] = 10^{-2}$; molar ratios of AA : BA = 90 : 10 and AA : 1,4-dioxane = 1.0 : 1.5; $T = 80^\circ\text{C}$.

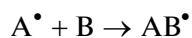
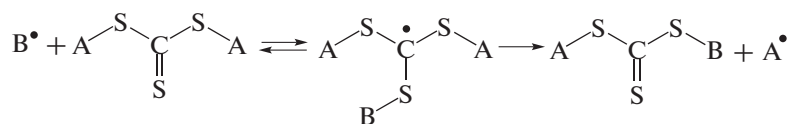
Another important criterion that the RAFT mechanism is implemented in the system is the width of MWD, the quantitative measure of which may be dispersion over molecular weight \bar{D} . Figure 4 presents the plots of dispersion as a function of conversion for the synthesized copolymers. It is seen that the copolymers formed in solution are characterized by a fairly narrow MWD ($\bar{D} < 1.3$). When copolymerization is carried out in bulk, the values of \bar{D} are higher; however, they are nevertheless lower than those for the copolymers synthesized by conventional radical copolymerization.

Thus, we showed for the first time that the AA–BA amphiphilic copolymers with a narrow MWD and controlled MW can be synthesized directly by the BTC-mediated RAFT copolymerization. For further studies 1,4-dioxane was chosen as a solvent because it is thermodynamically good for both homopolymers and the monomer feed containing 90 mol % AA.

Figure 5 shows the composition of the copolymer obtained from this comonomer mixture as a function of the total conversion of the monomers. It is seen that the experimental values of the molar fraction of AA in the copolymer (dark symbols) are in good agreement with the data calculated using the reactivity ratios (the straight line). Note that, when a monomer conversion of ~20% is attained, the average composition of the copolymer remains almost unchanged and close to the composition of the monomer feed. Thus, under the chosen conditions, the copolymerization yields the random copolymer with narrow MWD.

Symmetric Random Triblock Copolymers A–block–(A/B)–block–A and B–block–(A/B)–block–B

Polymeric RAFT agents synthesized in the presence of symmetric trithiocarbonate, BTC, contain the trithiocarbonate fragment within the chain and have the structure $A-S-C(=S)-S-A$, where A is the polymeric substituent. The introduction of such a polymeric RAFT agent in the copolymerization of monomers A and B initiated by the radical initiator AIBN causes the generation of radicals with terminal unit A^\bullet or B^\bullet and their addition to the polymeric RAFT agent. The interaction of the polymeric RAFT agent with radical A^\bullet occurs in a manner similar to that of reaction (3). The reaction of the polymeric RAFT agent with radical B^\bullet gives rise to an intermediate, for which the direction of fragmentation is determined by the nature of substituents A and B. In this case, for the RAFT mechanism to be realized, the polymeric substituent A of the initial polymeric RAFT agent should be split off during fragmentation and then it should initiate the polymerization of monomer B:



As a result of the repeated RAFT reactions, the structure of the polymerization product, provided the reaction conditions are chosen correctly [23], will be as follows: *A-block-(A/B)-block-A* or *A-(A/B)-S-C(=S)-S-(A/B)-A*.

With consideration for the above data, it can be anticipated that, when using both types of RAFT agents (PAATC and PBATC), the copolymerization of AA and BA will yield random block copolymers with a narrow MWD.

The time dependences of conversion obtained for the copolymerization of AA and BA mediated by

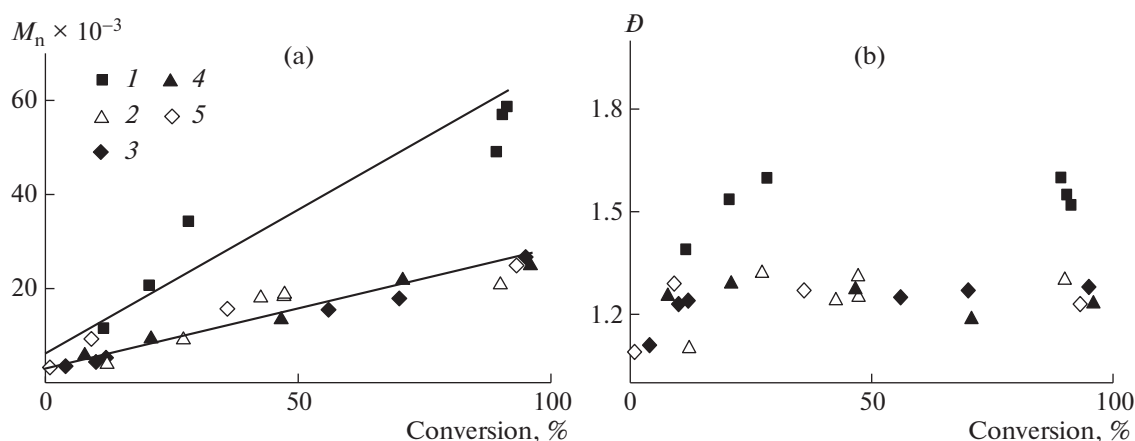


Fig. 4. Dependences of (a) M_n and (b) D of the copolymers on monomer conversion for the copolymerization of AA and BA at 80°C, $[AIBN] = 10^{-3}$ mol/L and $[BTC] = 10^{-2}$ mol/L; molar ratio of AA : BA = (1–3) 68 : 32 and (4, 5) 90 : 10; (1) in bulk, (2, 4) 1,4-dioxane, and (3, 5) DMF.

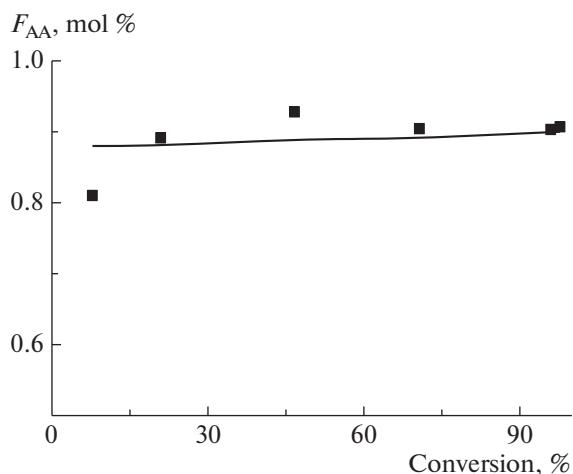


Fig. 5. Dependence of the molar fraction of AA units in copolymer F_{AA} on comonomer conversion for the BTC-mediated copolymerization of AA and BA in 1,4-dioxane at 80°C. $[AIBN] = 10^{-3}$ mol/L and $[BTC] = 10^{-2}$ mol/L; molar ratios of AA : BA = 90 : 10 and AA : 1,4-dioxane = 1.0 : 1.5. See text for explanations.

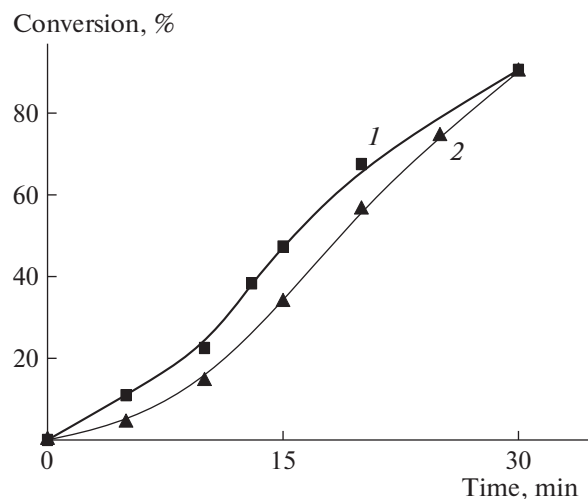
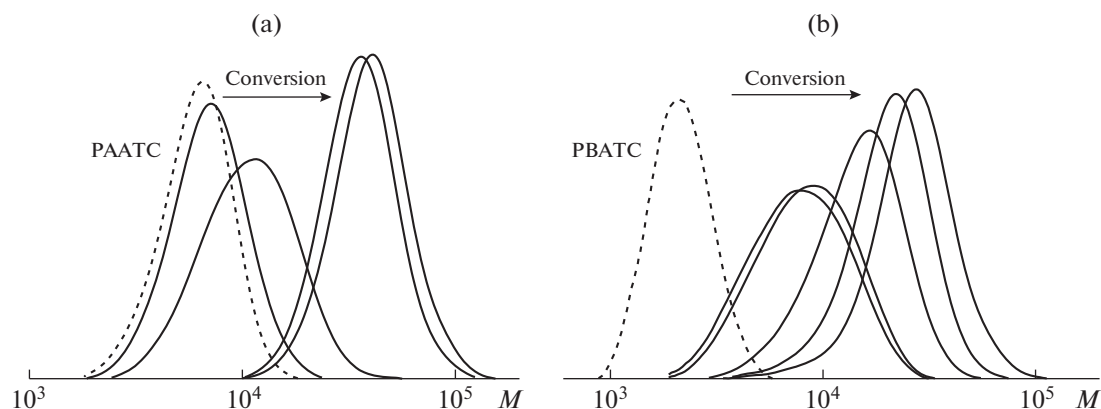


Fig. 6. Time dependence of conversion for the copolymerization of AA and BA in dioxane. $[AIBN] = 10^{-3}$ mol/L and $[PAATC] = [PBATC] = 10^{-2}$ mol/L; molar ratio of AA : BA = 90 : 10; RAFT agent: (1) PAATC and (2) PBATC. $T = 80^\circ\text{C}$.



1 **Fig. 7.** GPC curves of the products of copolymerization AA and BA in 1,4-dioxane. $[AIBN] = 10^{-3}$ mol/L and $[PAATC] = [PBATC] = 10^{-2}$ mol/L; molar ratio of AA : BA = 90 : 10; RAFT agent: (a) PAATC and (b) PBATC. $T = 80^{\circ}\text{C}$.

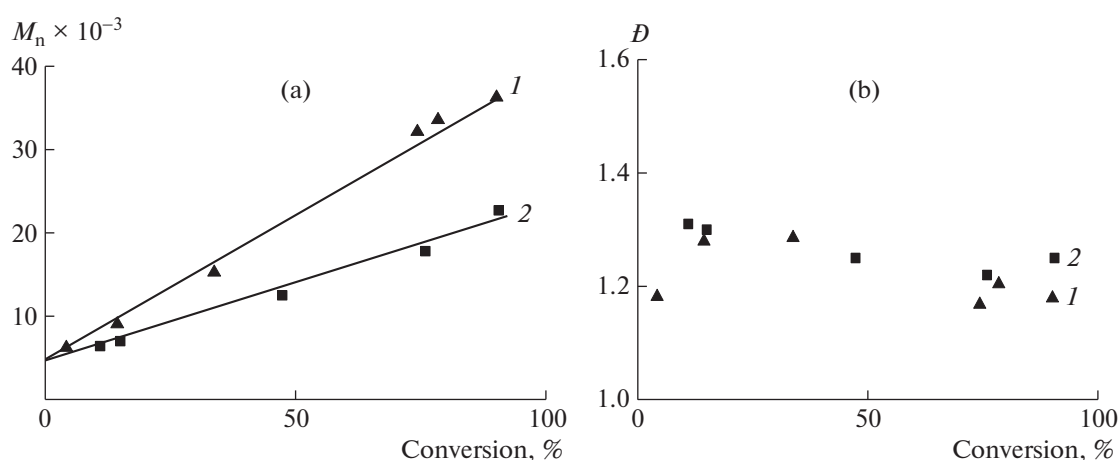


Fig. 8. Dependences of (a) M_n and (b) D of copolymers on comonomer conversion for the copolymerization of AA and BA in 1,4-dioxane. $[AIBN] = 10^{-3}$ mol/L and $[PAATC] = [PBATC] = 10^{-2}$ mol/L; molar ratio of AA : BA = 90 : 10; RAFT agent: (1) PAATC and (2) PBATC. $T = 80^{\circ}\text{C}$.

PAATC and PBATC are shown in Fig. 6. It is seen that, under the chosen conditions, copolymerization proceeds at a high rate and ultimate conversions ($\sim 90\%$) are attained within half an hour. The nature of the polymeric RAFT agent insignificantly affects the kinetics of the process.

The polymeric RAFT agents show high efficiency in the copolymerization of AA and BA. As is clear from Fig. 7, with an increase in the conversion of the comonomers, the introduced RAFT agents (PAATC and PBATC) are consumed completely and the polymers with a unimodal MWD are formed. In the course of polymerization, the MWD curve of the reaction product shifts to higher molecular weights. The number-average molecular weight of the copolymers increases linearly with the comonomer conversion, and a fairly low dispersion is preserved (Fig. 8). Different slopes of the conversion dependences of M_n

(Fig. 8a) are apparently associated with the error in the determination of MW values for the original polymeric RAFT agents of different chemical nature according to PMMA standards and, as a consequence, the error in the calculation of their concentrations in the synthesis of the copolymers.

The formation of polymers with a narrow MWD with the use of the polymeric RAFT agent makes it possible to state that the polymerization products are block copolymers. Their composition was studied by the conductometric titration, and, according to these data, the total fraction of acrylic acid in the reaction product and its content in the copolymer "grown" on the polymeric RAFT agent were calculated (Fig. 9). It is obvious that the average compositions of the copolymers at the initial and average conversions are different owing to the contribution of polymeric RAFT agents, PAATC and PBATC. At the same time, at high

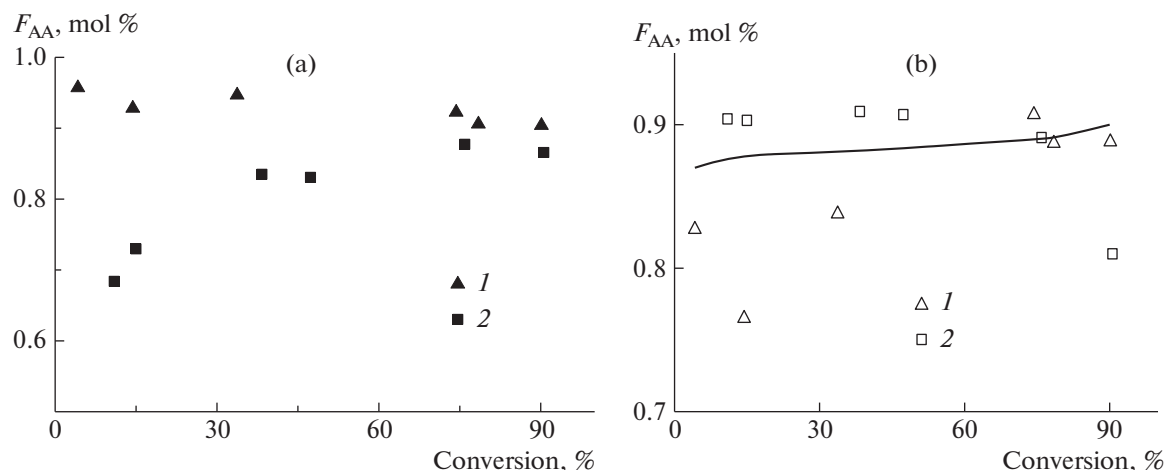


Fig. 9. Dependences of (a) the total molar fraction of AA units and (b) the molar fraction of AA in the “grown” copolymer on comonomer conversion for the copolymerization of AA and BA mediated by (1) PAATC and (2) PBATC. $[AIBN] = 10^{-3}$ mol/L and $[PAATC] = [PBATC] = 10^{-2}$ mol/L; molar ratio of AA : BA = 90 : 10; $T = 80^{\circ}\text{C}$. See text for explanations.

conversions, the average compositions of copolymerization products are similar for the monomer feed of the same composition.

However, the compositions of the “grown” copolymers are different. It is seen that they differ not only from the theoretical composition (calculated from the reactivity ratios determined for the two copolymers synthesized with the use of BTC) but also from each other. An analogous result was previously reported for the copolymerization of AA and styrene mediated by hydrophilic and hydrophobic polymeric RAFT agents; it was attributed to the effect of selective solvation of the monomers [10, 12].

According to the above evidence, it can be stated that, with the use of polymeric RAFT agents PAATC and PBATC, it is possible to synthesize the random block copolymers with a narrow MWD and different chain microstructures.

Taking into account the kinetic features of copolymerization, three copolymers were synthesized with participation of BTC, PAATC, and PBATC using monomer feeds containing 90 mol % acrylic acid. The characteristics of the products are listed in Table 2. It is clear that the compositions of the “grown” copolymers are similar; all the copolymers contain ~90 mol % AA units. The total compositions of the copolymers, their average MW values, and dispersions are comparable. At the same time, the copolymers are distinguished by the microstructures of macromolecules: copolymer 1 is a random copolymer (320 units); in copolymer 2, the random copolymer (390 units) is chemically bound from both ends to two hydrophilic PAA blocks with a length of ~40 units; and in copolymer 3, the random copolymer (250 units) is chemically bound to two hydrophobic PBA blocks with a length of ~10 units.

Let us consider how chain composition and microstructure influence the properties of the copolymers in the solid state and in dilute aqueous solutions.

Properties of Amphiphilic Copolymers in the Solid Phase

Figure 10 presents the thermograms of copolymers 1–3 in the solid state. The appearance of “steps” on the temperature dependences of heat flow (marked by arrows in Fig. 10) indicates devitrification of the copolymers, and the temperature of the inflection point corresponds to the glass transition temperature T_g . For all three samples, the thermograms show only one step with glass transition temperatures of $+116^{\circ}\text{C}$ (copolymers 1, 2) and $+118^{\circ}\text{C}$ (copolymer 3), which differ appreciably from the glass transition temperatures of individual homopolymers: PBA ($T_g \sim -55^{\circ}\text{C}$) and PAA ($T_g \sim +106^{\circ}\text{C}$) [22].

The finding that the glass transition temperatures of the random block copolymers and their random analog are almost coincident makes it possible to assign the detected temperature transition to devitrification of the $(AA/BA)_n$ block. The absence of glass transition temperatures of individual PAA (copolymer 2) and PBA blocks (copolymer 3) on the thermograms can be explained by their small weight contribution to the copolymer (14–15 wt %). In the solid state, these blocks are “squeezed” in the matrix of the random copolymer and cannot pass to the rubbery state before devitrification of a more massive block $(AA/BA)_n$.

The glass transition temperature of the random block in the studied copolymers calculated by the Flory–Fox equation $\frac{1}{T_g} = \frac{\omega_1}{T_{g,1}} + \frac{\omega_2}{T_{g,2}}$ (T_g is the glass transition temperature of the copolymer, $T_{g,1}$ and $T_{g,2}$

Table 2. Composition and molecular weight characteristics of the AA–BA copolymers synthesized using various RAFT agents

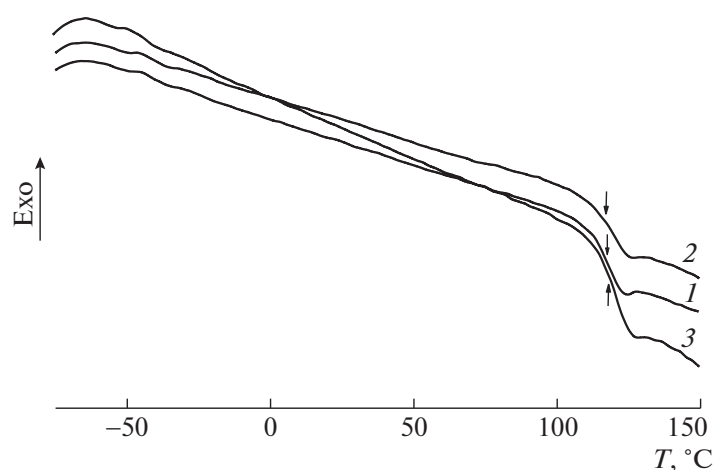
Copolymer	RAFT agent	Content of AA*, mol %		$M_n \times 10^{-3}$	\bar{D}	Microstructure
		total	“grown”			
1	BTC	90.3	90.3	24.9	1.20	–(AA/BA) _n –
2	PAATC	90.4	88.8	36.3	1.18	PAA–(AA/BA) _n –PAA
3	PBATC	86.6	91.1	22.7	1.23	PBA–(AA/BA) _n –PBA

* Conductometric titration data.

are the glass transition temperatures of homopolymers PAA and PBA, and $\omega_1 = 0.82$ – 0.85 and $\omega_2 = 0.15$ – 0.18 are the weight fractions of AA and BA units in the copolymer) is in the range of 62 – 68°C . The calculated values are much smaller than those obtained in experiments. In other words, the antiplasticizing effect of BA units on AA units is observed, which is manifested in the fact that the glass transition temperature of the copolymer increases by almost 10°C relative to the glass transition temperature of the pure PAA. Note that an analogous effect was described for the block copolymers of PAA with PS and PAA with PBA [24]. For example, for the block copolymer $\text{PBA}_{10200}\text{PAA}_{2900}$ (subscripts below designate the molecular weight of respective blocks), the glass transition temperature of the PAA block increases to $+110^\circ\text{C}$; for the block copolymer $\text{PS}_{6200}\text{PAA}_{11500}$, it increases to $+139^\circ\text{C}$. It may be assumed that an increase in the glass transition temperature of the random block AA/BA relative to that of the pure PAA is related to enhancement of the dipole–dipole interaction of AA units as a result of reduction in the dielectric permittivity of the medium in the presence of BA nonpolar units. As a consequence, the kinetic flexibility of polymer chains decreases and this makes itself evident as a rise in the glass transition temperature.

Figure 11 shows photographs of a water droplet on the surface of copolymer films formed by drying their aqueous solutions (1 – 2 wt %) on Teflon or glass substrates. Note that for both substrates the contact angles are close or coincide. This indicates a good adhesion of the copolymer to both types of materials and a full coverage of the substrate surface by the copolymer film. The photographs demonstrate that in all cases the water droplet spreads well over the copolymer film and the contact angles are acute, suggesting the hydrophilicity of the film. This result is expected taking into account a high content of AA units (87 – 90 mol %) in the copolymers. For copolymers 1 and 2 with the same total composition, the contact angles are almost coincident and amount to 35° – 40° ; the presence or absence of the PAA block has no effect on the wettability of the films. For copolymer 3, these angles are larger (45°). It is reasonable to attribute this fact to an increase in the total content of nonpolar BA units in the copolymer (Table 2).

Thus, our study of the bulk and surface properties the copolymers revealed that they are similar to the properties of PAA. The copolymers are hydrophilic, and their glass transition temperature is close to the glass transition temperature of the pure PAA. At the same time, the glass transition temperature of the

**Fig. 10.** Thermograms of copolymers 1–3 registered at a heating rate of $10^\circ\text{C}/\text{min}$. The glass transition temperatures are marked by arrows. The numbering of the curves corresponds to the numbering of the samples in Table 2.

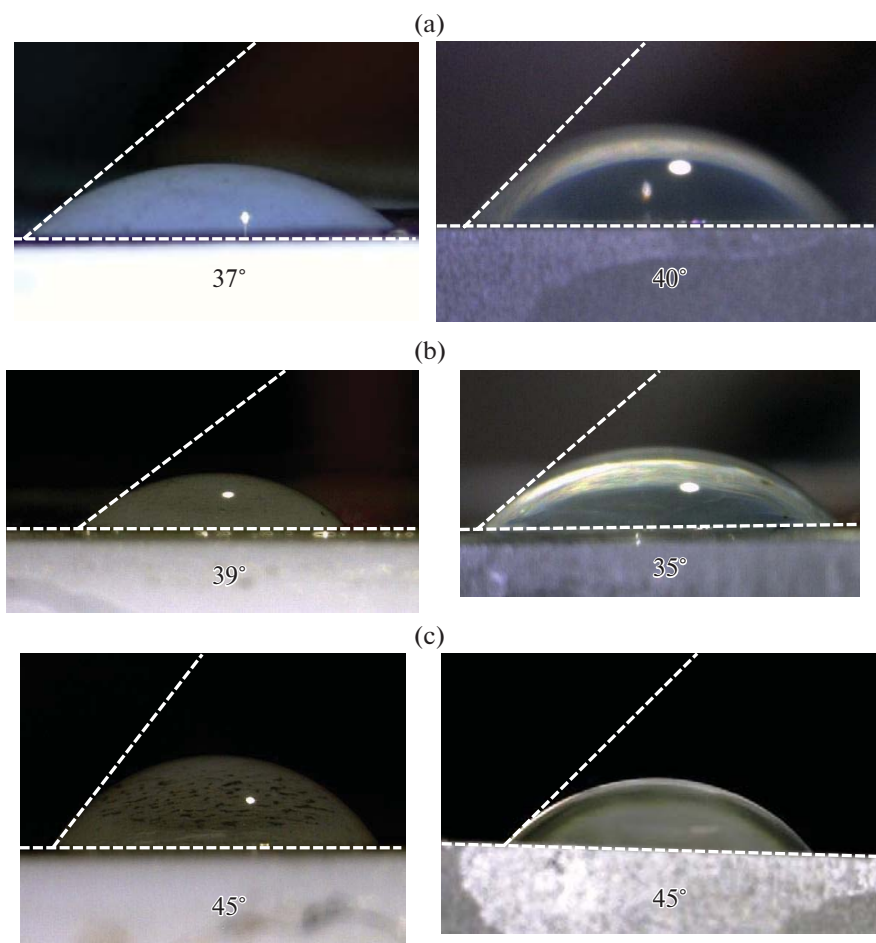


Fig. 11. (Color online) Photographs of films of copolymers (a) 1, (b) 2, and (c) 3 with the water droplet applied on them. The fluoroplastic substrate is on the left, and the glass substrate is on the right. Contact angle values are shown under the photographs.

copolymers is higher and they (as opposed to PAA) do not undergo spontaneous dispersion in water. In other words, even a small percent of BA units can substantially change the properties of polyacid. It makes sense to assume that this effect will be more pronounced in aqueous media, where the hydrophobic interactions of nonpolar units and the electrostatic interactions of dissociating ionic units come into play. Let us consider this case in more detail.

Properties of AA–BA Copolymers in Dilute Aqueous Solutions

The numerical distribution curves of scattered light intensity amplitude over the diameter of particles d for copolymers 1–3 in dilute aqueous solutions at inherent pH values show a single maximum. This suggests that only one type of polymer particles is present in solution. The number-average diameter of the particles is ~ 80 nm (copolymer 1), 4 nm (copolymer 2), and 13 nm (copolymer 3).

The aggregative state of macromolecules in a certain solvent may be evaluated from the average hydrodynamic diameter of particles D_h when comparing it with the assumed sizes of the Gaussian or completely unfolded macromolecular coil. The sizes of the unfolded macromolecular coil are characterized by its contour length L , and the sizes of the Gaussian coil in the unperturbed state are characterized by the rms end-to-end distance ($\langle h^2 \rangle_\Theta^{1/2}$). The contour length of a chain may be calculated as $L = Pl_{\text{unit}}$, where l_{unit} is the length of the monomer unit, which is equal to 0.25 nm for vinyl polymers, and P is the degree of polymerization. The unperturbed sizes of the copolymers may be approximately assessed by the empirical equation obtained for PAA: $\langle h^2 \rangle_\Theta = 6.7 \times 2P \times l_{\text{bond}}^2$, where l_{bond} is the length of the C–C bond equal to 0.154 nm [22]. In this case, the hydrodynamic diameter of the coil in the unperturbed state $(D_h)_\Theta$ can be calculated as $(D_h)_\Theta = 2\langle h^2 \rangle_\Theta^{1/2} / (1.5\sqrt{6})$.

For copolymer 1 the obtained values are as follows: $L \sim 80$ nm and $(D_h)_\Theta \sim 5.5$ nm. In order of magnitude, the experimentally observed effective hydrodynamic diameter $(D_h)_{\text{eff}}$ equal to ~ 80 nm is close to the contour length. However, it is unlikely that a fairly long weakly charged flexible-chain polymer will adopt the rodlike conformation. Therefore, the effective hydrodynamic diameter of the particles obtained for the random copolymer AA/BA may be attributed to the formation of intermacromolecular associates of the copolymer. The reason behind association is interchain hydrophobic interactions between nonpolar BA units.

For copolymer 2, we have $L \sim 117$ nm, $(D_h)_\Theta \sim 6.6$ nm, and $(D_h)_{\text{eff}} \sim 4$ nm. It is seen that, in order of magnitude, the sizes of polymer particles for copolymer 2 are similar to the sizes of individual coils; i.e., in aqueous solutions, the random block copolymer PAA-(AA/BA)-PAA is dispersed to the level of individual macromolecules.

Finally, for copolymer 3, we arrive at the following values: $L \sim 70$ nm, $(D_h)_\Theta \sim 5.1$ nm, and $(D_h)_{\text{eff}} \sim 13$ nm. The sizes of polymer particles in this case cannot be attributed to either individual coils or associates. Allowing for the presence of two PBA blocks and the tendency of amphiphilic block copolymers to micellization [8, 25], it is reasonable to propose that micelles with the PBA core and the amphiphilic AA/BA corona are formed.

Thus, copolymers 1–3 of similar composition demonstrate different aggregative behavior during dispersion in water: the formation of individual coils (PAA-(AA/BA)-PAA), micelles (PBA-(AA/BA)-PBA), or large intermacromolecular associates (AA/BA). These discrepancies are associated with different microstructures of the studied copolymers. The presence of two terminal hydrophilic PAA blocks stabilizes the coil conformation and prevents the intermacromolecular association, while the presence of two terminal hydrophobic PBA blocks “directs” this association to the formation of polymer micelles.

Let us consider how the difference in the aggregative states of the copolymers affects their dispersion stability with a change in the thermodynamic quality of the solvent. The thermodynamic quality of the solvent with respect to AA units may be improved by alkalization of solution and may be worsened by its acidification. The phase behavior of copolymer solutions was analyzed by the turbidimetric titration with 0.1 M NaOH or 0.1 M HCl aqueous solution. The introduction of alkali causes the ionization of AA units, improves the thermodynamic quality of the solvent with respect to the copolymers, and enhances their dispersion stability. This makes itself evident as the invariability or reduction in the optical density of solutions with an increase in pH.

The addition of HCl, on the contrary, suppresses the dissociation of AA units and worsens the thermodynamic quality of the solvent. Figure 2 shows the

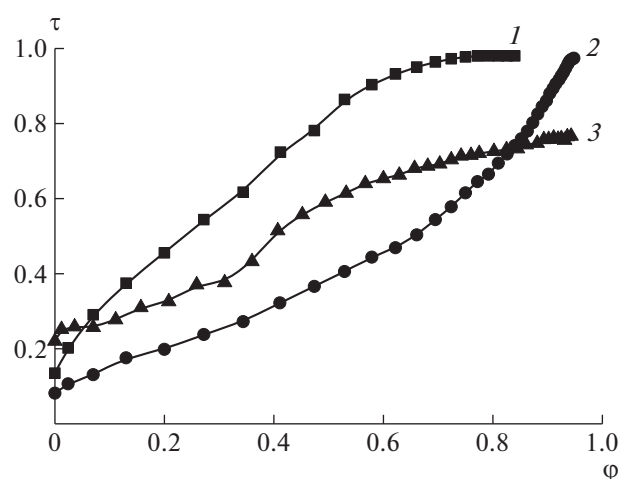


Fig. 12. Turbidity τ of the aqueous solutions of copolymers 1–3 vs. the volume fraction of 0.1 M HCl aqueous solution ϕ . The numbering of the curves corresponds to the numbering of the samples in Table 2.

dependences of turbidity τ of the aqueous solutions of the copolymers on the volume fraction of 0.1 M HCl ϕ . It is seen that, for all the copolymers, the turbidity of the medium monotonically increases. This fact provides evidence for the progressing loss of dispersion stability by the copolymers and the isolation of polymer particles into the concentrated phase. In a wide range of ϕ values, the turbidity changes as follows: τ (copolymer 1) $>$ τ (copolymer 3) $>$ τ (copolymer 2). This trend reflects the difference in the average sizes of the precipitating particles of the new phase (the larger the sizes, the higher the turbidity) and correlates well with the observed difference in the hydrodynamic sizes of the copolymer particles at the inherent pH value.

Different microstructures and aggregative states of the copolymers may appear as different natures of the acidic dissociation of their macromolecules, because the local environment of carboxyl groups and their local concentration in particles will be different. Figure 13a shows the potentiometric titration curves of the copolymers with the NaOH solution plotted in coordinates pH–degree of dissociation α . For comparison, the potentiometric titration curve is obtained for PAATC. These dependences are used for estimating the effective constants for the acidic dissociation of carboxyl groups pK_a (Fig. 13b).

It is seen that, at $\alpha < 0.3$, the dependences of pK_a on α for the copolymers are situated above the respective dependence for PAATC. To determine the characteristic constant pK_0 corresponding to ionization of the first proton, the dependences of pK_a on α were extrapolated to the zero degree of ionization. The values of pK_0 were 4.9, 4.8, and 4.8 for copolymers 1, 2, and 3, respectively, and 4.5 for PAATC. This result indicates that the copolymer acids are weaker polyac-

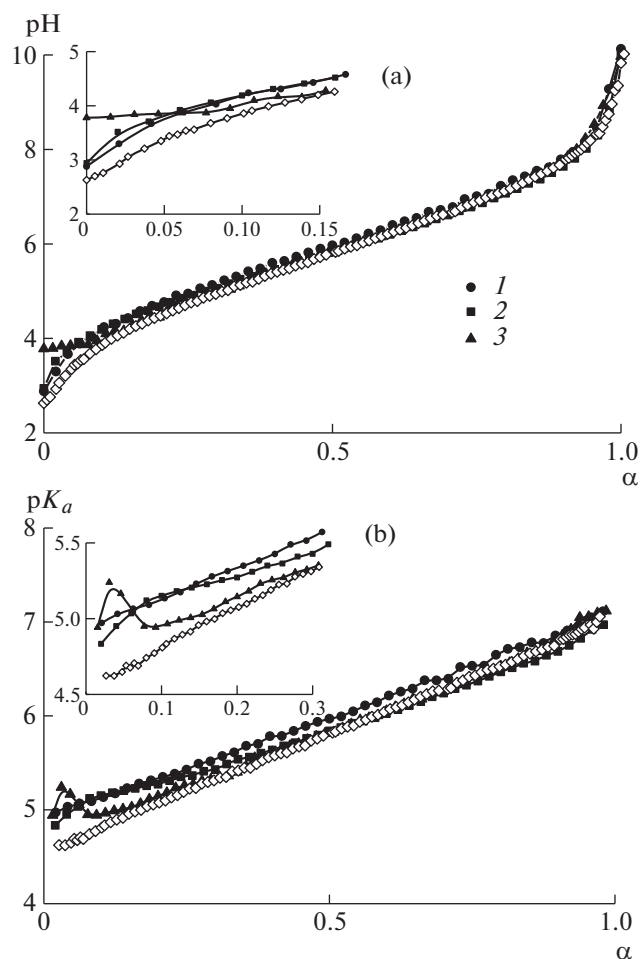


Fig. 13. (a) Titration curves of aqueous copolymer solutions and (b) dependences of pK_a on the degree of association α . The numbering of the curves corresponds to the numbering of the samples in Table 2. Open symbols correspond to PAATC. See text for explanations.

ids than the pure PAA. The reason behind the weakened strength of acids may be reduction in the local dielectric permittivity of polymer particles related to the presence of nonpolar BA units.

In contrast to an almost linear dependence of pK_a on α for PAATC and copolymer 1, the dependence of pK_a on α for copolymer 2 increases nonmonotonically in the range $0 < \alpha < 0.2$. An even more concave nature of the plot of pK_a as a function of α is expressed for copolymer 3 in the range $0 < \alpha < 0.1$. The nonmonotonic pattern of the dependence of pK_a on α is well known for polyacids with the secondary structure, for example, poly(methacrylic acid) [26–28] or poly(glutamic acid) [29, 30], and suggests that the conformational transition occurs upon the ionization of polyacid. For example, for poly(methacrylic acid), this is the transition from the compact conformation stabilized by the hydrophobic interactions of methyl groups

and the hydrogen bonding of carboxyl groups to the coil one [26–28].

It is logical to suppose that, for copolymer 2, we also deal with the conformational transition from the compact conformation to the coil one during ionization. Compaction of the coil at low α values may be provided by the intramolecular hydrophobic interactions of butyl acrylate units. The ionization of polyacid leads to a rise in the electrostatic energy of repulsion between carboxyl groups, which is accompanied by destruction of the compact conformation. In the case of copolymer 1, the interchain association of butyl acrylate units prevails; therefore, the compaction of coils is absent.

For copolymer 3 at low values of α , there is the compaction of AA/BA blocks in the corona of the micelle due to the hydrophobic association of BA units. This compaction results in the formation of micelles with the compressed AA/BA corona. Similar micelles were described in [9]. According to the authors of [9], an increase in the content of charged units above a certain threshold value causes an “abrupt” unfolding of the corona and the destruction of its compact conformation. It is reasonable to assume that in our case such a conformational transition takes place during the ionization of AA units in the course of titration.

CONCLUSIONS

Our studies showed that the RAFT polymerization technique may be an effective tool for the targeted introduction of hydrophobic units into a polyelectrolyte chain. The use of the low molecular weight RAFT agent (BTC) or polymeric RAFT agent (PAATC or PBATC) enables one to vary the percentage of hydrophobic units and the pattern of their distribution (random or random block copolymers with terminal ionic or low-polarity blocks of the predetermined length). Such copolymers with a similar average composition have similar properties in the bulk or on the surface of the solid phase (the glass transition temperature, wettability); however, during dispersion in aqueous media, their aggregative behavior and the character of distribution of electrolyte units become different. Our synthetic approach makes it possible to tune the behavior of hydrophobically modified polyelectrolytes in aqueous media, which may open new areas for the practical application of well-known and mass-produced PAA-type polyelectrolytes.

FUNDING

This work was supported by the Russian Foundation for Basic Research (project no. 17-03-00131a).

REFERENCES

1. M. Nagasawa, *Physical Chemistry of Polyelectrolyte Solutions* (Wiley, Malden, 2015).
2. *Polyelectrolytes: Thermodynamics and Rheology*, Ed. by P. M. Visakh O. Bayraktar, and G. A. Pico (Springer, Berlin, 2014).
3. *Polyelectrolyte Complexes in the Dispersed and Solid State II: Application Aspects*, Ed. by M. Muller (Springer, Berlin, 2014).
4. A. B. Zezin, S. V. Mikheikin, V. B. Rogacheva, M. F. Zansokhova, A. V. Sybachin, and A. A. Yaroslavov, *Adv. Colloid Interface Sci.* **226**, 17 (2015).
5. J. Kotz, S. Kosmella, and T. Beitz, *Prog. Polym. Sci.* **26**, 1199 (2001).
6. P. Raffa, D. A. Z. Wever, F. Picchioni, and A. A. Broekhuis, *Chem. Rev.* **115**, 8504 (2015).
7. A. M. Pedley, J. S. Higgins, D. G. Peiffer, and A. R. Rennie, *Macromolecules* **23**, 2494 (1990).
8. O. V. Borisov, E. B. Zhulina, F. A. M. Leermakers, and A. H. E. Muller, *Adv. Polym. Sci.* **241**, 57 (2011).
9. E. A. Lysenko, A. I. Kulebyakina, P. S. Chelushkin, A. M. Rumyantsev, E. Yu. Kramarenko, and A. B. Zezin, *Langmuir* **28**, 17108 (2012).
10. D. V. Vishnevetskii, A. V. Plutalova, V. V. Yulusov, O. S. Zotova, E. V. Chernikova, and S. D. Zaitsev, *Polym. Sci., Ser. B* **57**, 197 (2015).
11. N. S. Serkhacheva, O. I. Smirnov, A. V. Tolkachev, N. I. Prokopov, A. V. Plutalova, E. V. Chernikova, E. Yu. Kozhunova, and A. R. Khokhlov, *RSC Adv.* **7**, 24522 (2017).
12. E. V. Chernikova, S. D. Zaitsev, A. V. Plutalova, K. O. Mineeva, O. S. Zotova, and D. V. Vishnevetsky, *RSC Adv.* **8**, 14300 (2018).
13. A. Grigoreva, E. Polozov, and S. Zaitsev, *Colloid Polym. Sci.* **297**, 1423 (2019).
14. E. V. Chernikova, P. S. Terpugova, E. S. Garina, and V. B. Golubev, *Polym. Sci., Ser. A* **49**, 108 (2007).
15. E. V. Chernikova, A. Morozov, E. Leonova, E. Garina, V. Golubev, Ch. Bui, and B. Charleux, *Macromolecules* **37**, 6329 (2004).
16. E. V. Chernikova, P. S. Terpugova, M. Yu. Trifilov, E. S. Garina, V. B. Golubev, and E. V. Sivtsov, *Polym. Sci., Ser. A* **51**, 658 (2009).
17. E. A. Egorova, V. P. Zubov, I. V. Bakeeva, E. V. Chernikova, and E. A. Litmanovich, *Polym. Sci., Ser. A* **55**, 519 (2013).
18. E. V. Chernikova, A. V. Plutalova, K. O. Mineeva, I. R. Nasimova, E. Yu. Kozhunova, A. V. Bol'shakova, A. V. Tolkachev, N. S. Serkhacheva, S. D. Zaitsev, N. I. Prokopov, and A. B. Zezin, *Polym. Sci., Ser. B* **57**, 547 (2015).
19. E. V. Chernikova, N. S. Serkhacheva, O. I. Smirnov, N. I. Prokopov, A. V. Plutalova, E. A. Lysenko, and E. Yu. Kozhunova, *Polym. Sci., Ser. B* **58**, 629 (2016).
20. N. Serkhacheva, N. Prokopov, E. Chernikova, E. Kozhunova, O. Lebedeva, and O. Borisov, *Polym. Int.* **68**, 1303 (2019).
21. Yu. D. Semchikov and L. A. Smirnova, *Vysokomol. Soedin., Ser. B* **41**, 734 (1999).
22. *Polymer Handbook*, Ed. by J. Brandrup E. H. Immergut, and E. A. Grulke (Wiley, NewYork, 1999).
23. E. V. Chernikova and E. V. Sivtsov, *Polym. Sci., Ser. B* **59**, 93 (2017).
24. D. V. Vishnevetski, E. A. Lysenko, A. V. Plutalova, and E. V. Chernikova, *Polym. Sci., Ser. A* **58**, 1 (2016).
25. G. Reiss, *Prog. Polym. Sci.* **28**, 1107 (2003).
26. T. M. Birshtein, E. V. Anufrieva, T. N. Nekrasova, O. B. Ptitsyn, and T. V. Sheveleva, *Vysokomol. Soedin., Ser. A* **7**, 372 (1965).
27. M. Mandel, J. C. Leyte, and M. G. Stadhouder, *J. Phys. Chem.* **71**, 603 (1967).
28. L. Ruiz-Perez, A. Pryke, M. Sommer, G. Battaglia, I. Soutar, L. Swanson, and M. Geoghegan, *Macromolecules* **41**, 2203 (2008).
29. V. E. Bychkova, O. B. Ptitsyn, and T. V. Barskaya, *Biopolymers* **10**, 2161 (1971).
30. A. Godec and J. Skerjanc, *J. Phys. Chem. B* **109**, 13363 (2005).

Translated by T. Soboleva

SPELL: 1. dioxanee, 2. outgassed